Structural response of rectangular composite columns under vertical and lateral loads

Barış Sevim[*]

Yildiz Technical University, Department of Civil Engineering, 34220, İstanbul, Turkey

Abstract. The present study aims to determine the structural response of full scaled rectangular columns under both of vertical and lateral loads using numerical methods. In the study, the composite columns considering full concrete filled circular steel tube (FCFRST) and concrete filled double-skin rectangular steel tube (CFDSRST) section types are numerically modelled using ANSYS software. Vertical and lateral loads are applied to models to assess the structural response of the composite elements. Also similar investigations are done for reinforced concrete rectangular (RCR) columns to compare the results with those of composite elements. The analyses of the systems are statically performed for both linear and nonlinear materials. In linear static analyses, both of vertical and lateral loads are applied to models as only one step. However in nonlinear analyses, while vertical loads are applied to model as only one step, lateral loads are applied to systems as step by step. The displacement and stress changes in some critical nodes and sections and contour diagrams are reported by graphs and figures. At the end of the study, it is demonstrated that the nonlinear models reveal more accurate result then those of linear models. Also, it is highlighted that composite columns provide more and more safety, ductility compared to reinforced concrete column.

Keywords: composite column; finite element modeling; linear and nonlinear analyses; structural response; vertical and lateral loads thermal buckling; sandwich plate; functionally graded materials; plate theory

1. Introduction

The structural systems have been developed such as frame, shear wall, core, and tubular systems, respectively from 1900s to present, to build higher structures using conventional reinforced-concrete (RC). But the conventional material has limitation when building more strength, stiff, ductile, and durable structures. To elaborate the disadvantages RC systems, last two decades researchers have been started to study about the effectiveness of composite elements such as concrete filled steel tubes (CFST) on engineering structures, especially high-rise buildings and piers of the bridges (Sakino *et al.* 2004, Chen *et al.* 2008, Karimi *et al.* 2011, Patidar 2012, Liu 2013, Fakharifar *et al.* 2014, Wu *et al.* 2015, Huang *et al.* 2016, Aslani *et al.* 2016). Composite elements are economical materials and they provide quicker construction which makes more preferable than conventional RC elements. However, the main disadvantages of composite elements are the problems on the connection of complicated joint of column-RC beam and lower steel-fire and corrosion resistant. But the main reason of using these elements are specified as that higher axial load capacity, better ductility performance, larger energy absorption capacity, and lower strength degradation (Patidar 2012, Liu 2013, Gua *et al.* 2014, Oyowa *et al.* 2016, Pereira 2016, Zhao 2016). Steel tube as a part of composite element provides

confining effects to concrete to behave in a tri-axial compressive stress state while concrete prevents the steel tube for from buckling inward (Liu 2013, Fakharifar *et al.* 2014). Sakino *et al.* (2004) studied about the response of centrally loaded concrete-filled steel tube short columns. 114 stub columns were built including parameters for the tests as follows: tube shape, tube tensile strength, tube diameter-to-thickness ratio, and concrete strength. In the study, the stress-strain relations were plotted.

Chen *et al.* (2008) told about the design concepts of reinforced with concrete filled steel tubes to increase bearing capacity and seismic performance. The design concepts such as strengthening, composition, confinement, and superposition were featured in the study to obtain optimal composite columns.

Karimi *et al.* (2011) presented a paper considering test and models of fiber-reinforced polymer encased steel-concrete columns under compressive loading. In the content of the study, seven stub columns were built in the laboratory and tested. It is highlighted from the study that the developed systems should be used to increase load carrying capacity, axial stiffness and energy dissipation capacity of existing composite columns.

Liu (2013) presented a research which aims to investigate behavior of the concrete-filled steel tube with outer steel plank reinforced concrete stub columns. Three column specimens were tested under axial load to evaluate the ultimate strength of the composite columns. In the study, numerical analyses were also performed to support the experimental results.

Ajel and Abbas (2015) investigated the structural response of stub columns using experimental and numerical

---

*Corresponding author, Professor,
 E-mail: basevim@yildiz.edu.tr

studies. Totally 31 square and circular samples with dimensions 150 mm section width or diameter and 300 mm height were built and tested. Also numerical models were constituted using ANSYS software. In the modeling SOLID65 and SOLID45 were respectively used to represent concrete and steel tube. LINK8 element was used to consider steel bars. The results obtained from the study are showed that the convergence between numerical and experimental failure load varies from 2 to 15%.

Essopjee and Dundu (2015) tested concrete-filled double-skin circular tube columns to assess the performance. 32 samples prepared for different lengths, diameters and strength of the outer steel tubes and axially loaded until failure. New formulae are developed based on South African standards and Eurocode 4 to increase the load capacity of composite columns.

Beside the studies clearly presented above, there are some studies related to composite structures such as subjects that selection of composite section type under axial loads and structural response (Wei *et al.* 1995, Schneider 1998, Hajjar 2002, Alnahhal and Aref 2008, Uenaka *et al.* 2010, Remennikov and Kong 2016, Chacon 2015), bonding effects (Li and Hadi 2003, Bouazaoui *et al.* 2007, Ha *et al.* 2013, Robinson and Melby 2015).

When reviewed the literature and examined practice applications it is seen that the concrete filled steel tubes as composite elements have several section types. Some of these sections can be classified as given below:

- Full Concrete Filled Circular Steel Tubes (FCFCSTs), (Fig. 1(a)), (Liu 2013)
- Full Concrete Filled Rectangular Steel Tubes (FCFRSTs), (Fig. 1(b)), (Liu 2013)
- Concrete Filled Double-Skin Circular Steel Tubes (CFDSCSTs), (Fig. 1(c)), (Essopjee and Dundu 2015)
- Concrete Filled Double-Skin Rectangular-Circular Steel Tubes (CFDSRCSTs), (Fig. 1(d)), (Essopjee and Dundu 2015)
- Concrete Filled Double-Skin Rectangular Steel Tubes (CFDSRSTs), (Fig. 1(e)), (Essopjee and Dundu 2015)
- Reinforced Concrete Filled Circular Steel Tubes (RCFCSTs), (Fig. 1(f)), (Ajel and Abbas 2015)
- Reinforced Concrete Filled Rectangular Steel Tubes (RCFRSTs), (Fig. 1(g)), (Ajel and Abbas 2015)
- Reinforced Concrete Encased-Steel Profile Elements (RCESPEs), (Fig. 1(h)), (Karimi *et al.* 2011)
- Concrete Filled Steel Tubes with Steel Profile Elements (CFSTSPEs), (Fig. 1(i)) (Karimi *et al.* 2011)

The many regions in the world are earthquake-prone area, especially in California in United States, in Japan, in Indonesia and also in Turkey. So composite elements should be used to build structures in these regions. However the studies in the literature are generally related to assess behavior of scaled samples under axial loads and many of them do not include the behavior of full-scaled elements under lateral loads. So considering the importance of composite structures and the lack of literature, more studies

must be done to investigate the structural response. The present study aims to determine the structural response of full scaled composite columns under both of vertical and lateral loads using numerical methods. In the study, the composite columns considering FCFRST (Fig. 1(b)) and CFDSRST (Fig. 1(e)) section types are numerically modeled using ANSYS software. Vertical and lateral loads are applied to models to assess the structural response of the composite elements. Also similar investigations are done for reinforced concrete rectangular (RCR) columns to compare the results with those of composite elements. The analyses of the systems are statically performed for both linear and nonlinear materials. In linear static analyses, both of vertical and lateral loads are applied to models as only one step. However in nonlinear analyses, while vertical loads are applied to model as only one step, lateral loads are applied to systems as step by step. The displacement and stress changes in some critical nodes and sections and contour diagrams are reported by graphs and figures. Finally, this paper summarizes the structural response of two different section type composite columns and a rectangular reinforced concrete column.

2. General specifications for composite columns

A composite column is defined as a composite member subjected mainly to compression or to compression and bending according to Eurocode 4 (2004). In this study full concrete filled rectangular composites (FCFRCs) are investigated. So the specifications given here are related to subjected columns. Composite columns are used to increase, strength for a given cross sectional dimension; stiffness leading to reduced slenderness and buckling resistance; corrosion and fire resistance in the case of concrete encased columns. Also they provide a formwork for concrete filled steel tubes and economical solutions with regard to material costs. The materials type of steel and concrete should be changed when composite element is designed or built. Steel class can be selected from S235 to S460, and concrete can be varied from C20 to C50 for optimal composite elements. On the other hand, the steel contribution ratio δ must consider the Eq. (1).
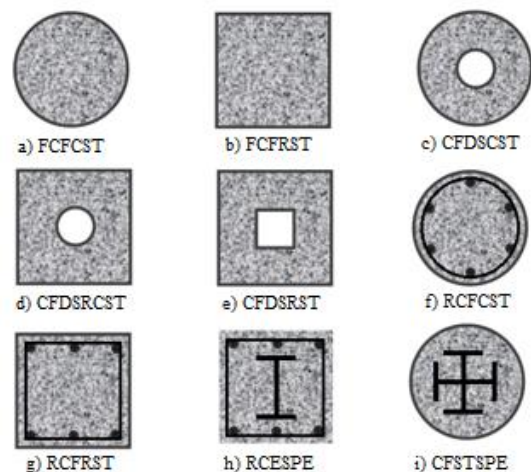

Fig. 1 Section types of composite structures

$$0.2 \leq \delta \leq 0.9 \text{ and } \delta = \frac{A_a f_{yd}}{N_{pl,Rd}} \qquad (1)$$

where, A_a cross-sectional area of the structural steel section, f_{yd} design value of the yield strength of structural steel, and $N_{pl,Rd}$ design value of the plastic resistance of the composite section to compressive normal force. In Eq. (1), $N_{pl,Rd}$ is assumed as in Eq. (2).

$$N_{pl,Rd} = A_a f_{yd} + \vartheta A_c f_{cd} + A_s f_{sd} \qquad (2)$$

where, ϑ buckling coefficient which can be selected as 1.0 for full concrete filled rectangular sections, A_c cross-sectional area of concrete, f_{cd} design value of the cylinder compressive strength of concrete, A_s cross-sectional area of reinforcement, and f_{sd} design value of the yield strength of reinforcing steel. Another design parameter relative slenderness λ is defined in Eq. (3).

$$\lambda = \sqrt{\frac{N_{pl,Rk}}{N_{cr}}} \leq 2.0 \qquad (3)$$

where, $N_{pl,Rk}$ characteristic value of the plastic resistance of the composite section to compressive normal force, and N_{cr} Elastic critical normal force. $N_{pl,Rk}$ is calculated using characteristics strengths instead of design strengths given in Eq. (2). The effects of buckling can be neglected for the steel section of FCFRC elements when providing the condition given in Eq. (4).

$$\frac{h}{t} \leq 52 \sqrt{\frac{235}{f_y}} \qquad (4)$$

where, h clear depth of the web of the steel tube (minimum transverse dimension of the column), t thickness of the steel tube, and f_y nominal value of the yield strength of structural steel.

3. Numerical examples

3.1 Description of the columns

In this study, a reinforced concrete rectangular (RCR) column, a full concrete filled rectangular steel tube (FCFRST) column, and a concrete filled double-skin rectangular steel tube (CFDSRST) column are selected for the numerical examples. The section of the columns are seen in Fig. 2, respectively. In the study, the height of the columns are selected as 3 m and both of width and depth of concrete part are assumed as 30 cm. Diameters of the longitudinal and tie bars in the reinforced concrete column are 14 and 8 mm, respectively. The wall thicknesses are considered as 6 and 3 mm, respectively for outer and inner steel tubes. The clear depth of the web of the steel tube (h) thickness of the steel tube (t) ratio is selected as 50 which is suitable to the literature and guidelines. Reinforced concrete rectangular (RCR) column considers 6 longitudinal bars with 14 mm diameters. These bars are confined with tie bars (8 mm diameter) along the height with 15 cm spans. However it is not assumed as special concrete confinement

through the steel tubes as you mean reinforced bars. The concrete-steel tube interaction surfaces are assumed as bounded. So it provides a confinement considered through the steel tubes. Steel tube as a part of composite element provides confining effects to concrete to behave in a tri-axial compressive stress state while concrete prevents the steel tube for from buckling inward. As materials, the concrete, reinforced bar and steel tube are selected as C30, S420, and ST37, respectively. Geometrical and material properties of the columns are listed in Tables 1 and 2, respectively. In the study, both of linear and nonlinear analyses are performed. So, Table 2 also considers the nonlinear material properties.

3.2 3D Finite Element Modeling of the Columns

3D finite element models of the columns (Fig. 3) are built by ANSYS (2016) software including geometrical and material properties listed in Tables 1 and 2. In the modeling; reinforced concrete rectangular (RCR) column is constituted using SOLID65 elements for concrete and LINK180 elements for reinforcement bars. Full concrete filled rectangular steel tube (FCFRST) column is constituted using SOLID65 elements for concrete and SOLID185 elements for outer steel tubes. Concrete filled double-skin rectangular steel tube (CFDSRST) column is constituted using SOLID65 elements for concrete and SOLID185 elements for outer and inner steel tubes.

SOLID65 element has 8 nodes, with each node having three translational degrees of freedom and it is capable of cracking in tension and crushing in compression. It is generally used for the three-dimensional modeling of solids with or without reinforced bars (ANSYS 2016).
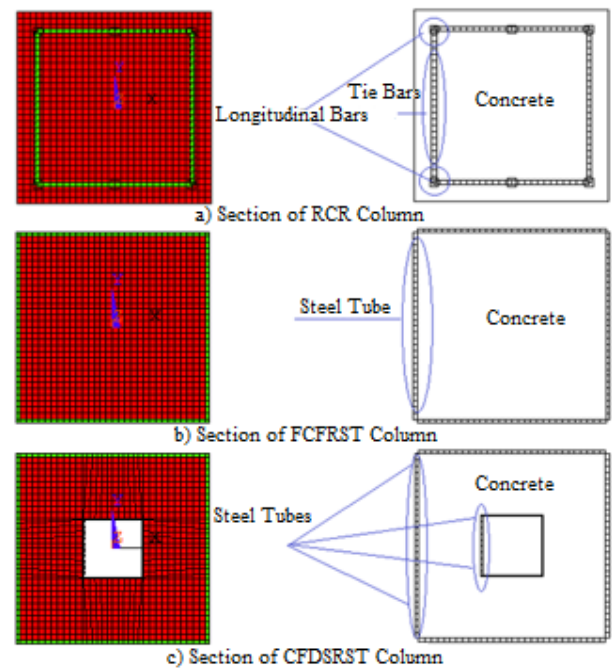

Fig. 2 Section of (a)RCR, (b)FCFRST and (c)CFDSRST columns

Table 1 Geometrical properties of the columns

Geometrical Properties	Columns		
	RCR	FCFRST	CFDSRST
Depth of outer section (ho) (cm)	30	30	30
Width of outer section (bo) (cm)	30	30	30
Depth of inner section (hi) (cm)	-	-	10
Width of inner section (bi) (cm)	-	-	10
Thickness of outer tube (to) (mm)	-	6	6
Thickness of inner tube (ti) (mm)	-	-	3

Table 2 Materials properties of the columns

Material Properties	All Columns			
	Concrete	Bar	Outer Tube	Inner Tube
Weight per unit volume (kg/m^3)	2400	7850	7850	7850
Elasticity Modulus (N/m^2)	3E10	2.1E11	2.1E11	2.1E11
Poisson Ratio	0.2	0.3	0.3	0.3
Yield Strength (MPa)	30	420	235	235
Tangent Modulus (MPa)	-	21	21	21
Yield Strain	0.001	Automatically calculated by ANSYS		
Ultimate Strain	0.003	Automatically calculated by ANSYS		

LINK 180 is a uni-axial tension-compression element and it has 2 nodes, with each node having three translational degrees of freedom. It includes plasticity, creep, swelling, stress stiffening, and large deflection capabilities (ANSYS 2016). SOLID185 an eight-node solid element is used to simulate the steel plates of composite columns. The element is defined with eight nodes having three degrees of freedom at each node –translations in the nodal x, y, and z directions.

The element has plasticity, stress stiffening, large deflection, and large strain capabilities (ANSYS 2016).

In a composite column both the steel and concrete would resist the external loading by interacting together by bond and friction. Also, in the modelling of composite columns, interaction between concrete and steel tubes are defined as slip surface, frictional surface or bounded. Most of studies use bounded surface between steel tube and concrete. (Furlong 1997, Kachalev and Miller 2001, Jacobs and Hajjar 2010, Pecce and Ceroni 2010, Ajel and Abbas 2016, Kisala 2016, Patel and Lande 2016). In this study steel tube-concrete interaction is assumed as bounded. In bounded interaction, contact surface is wider and the concrete is completely in the steel tubes, that gives a beneficial confinement effect. And this interaction provides more stiffness, which is preferred for composite columns.

Mesh refinement studies are also undertaken for all three models to assess the optimum numbers of elements. The numbers of the elements which are deemed sufficient for yielding a series of numerically converged solutions are listed in Table 3. In the study, each finite element is connected to each other with nodal points without considering contact surfaces between individual concrete and steel tube units. In defining the boundary conditions, all degrees of freedom under the columns are assumed as fixed.

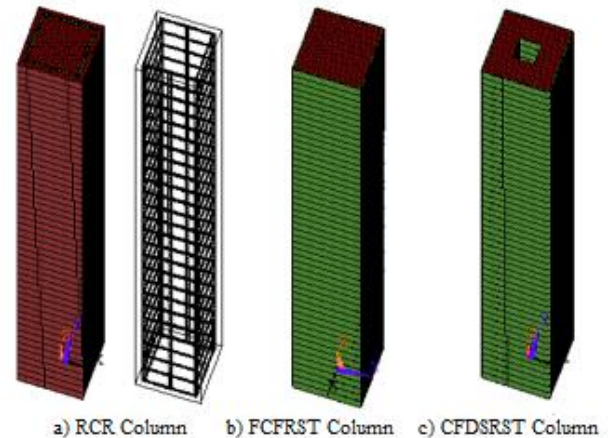a) RCR Column   b) FCFRST Column   c) CFDSRST Column

Fig. 3 3D finite element model of the columns

In the study, bilinear elastic behavior for concrete and bilinear kinematic hardening behavior (plastic behavior) for reinforced bars and steel tubes are assumed in nonlinear modeling and analysis. In bilinear elastic behavior, unloading occurs along the same path as loading. Successive slopes can be greater than the preceding slope; however, no slope can be greater than the elastic modulus of the material. The slope of the first curve segment usually corresponds to the elastic modulus of the material, although the elastic modulus can be input as greater than the first slope to ensure that all slopes are less than or equal to the elastic modulus. Yield strength, yield strain and ultimate strain values are assumed for concrete to represent the linear elastic behavior (see Table 2).

Table 3 Numbers of the elements used in the modeling

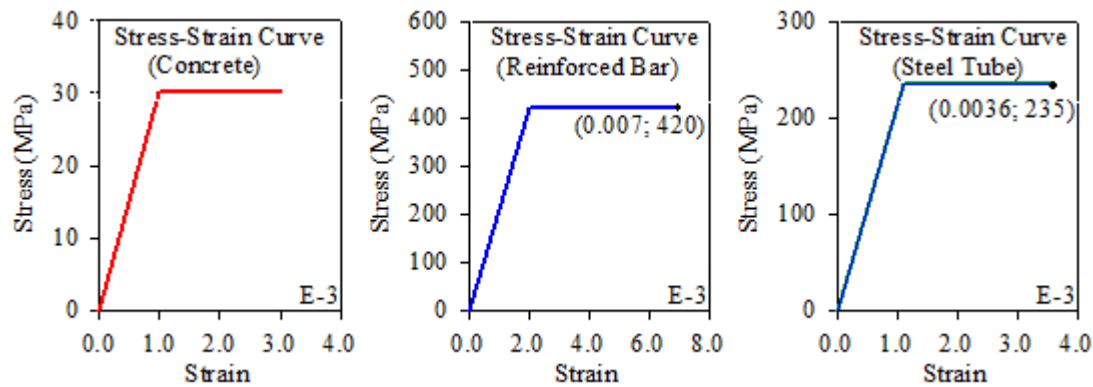| Element Type		Numbers of the Elements		
		RCR	FCFRST	CFDSRST
Concrete	SOLID65	45000	45000	44000
Reinforced Bar	LINK180	2796	-	-
Outer Steel Tube	SOLID185	-	6200	6200
Inner Steel Tube	SOLID185	-	-	2600

Fig. 4 Stress-strain curves for concrete, reinforced bar, and steel tube

In bilinear kinematic hardening behavior (plastic behavior), it is assumed the total stress range is equal to twice the yield stress. The material behavior is described by a bilinear total stress-total strain curve starting at the origin and with positive stress and strain values. The initial slope of the curve is taken as the elastic modulus of the material. Yield strength and tangent modules are assumed for reinforced bar and steel tube to represent the plastic behavior (See Table 2). Then yield and ultimate strain are automatically calculated by the software (see Fig. 4) (ANSYS, 2016). In nonlinear analyses of the study, stress-strain curve as bilinear elastic behavior for concrete and as bilinear kinematic hardening behavior for reinforced bar and steel tubes are plotted in Fig. 4.

3.3 Linear and Nonlinear Finite Element Analyses

In the study, linear and nonlinear analyses of the columns are performed using ANSYS (2016) software. Vertical and lateral static loads are applied to all models until the failure of materials. The vertical load is applied as pressure on the top area of the columns for only one step. Then under the initial conditions, lateral loads are applied to as single loads on all nodes at the top surface of the columns, and the size step is chosen as 0.0033 for nonlinear analyses. Nonlinear analyses consider both material and geometrical nonlinearities. The applied loads are listed in the Table 4.

Table 4 Values of vertical and lateral loads

Analyze	Loads	Columns		
		RCR	FCFRST	CFDSRST
Lin.	Vert.	30 MPa	30 MPa	30 MPa
	Lat.	85 kN	1520 kN	1620 kN
Nonlin	Vert.	30 MPa	30 MPa	30 MPa
	Lat.	85kN	1520 kN	1620 kN

K, L, and L' points and I-I section given as schematically in Fig. 5 are used to compare displacement and stress changing obtained from both linear and nonlinear analyses results of the models.

3.3.1 Finite element results of RCC column

In the finite element analyses, lateral loads are applied to model trough X direction. According to analyses results, the force-displacement curves and the changing of displacement along to height of the columns obtained from the analyses are presented in Figs. 6(a) and 6(b), respectively. As is seen in Fig. 6(a), displacements are about 25 mm and nearly same until 60 kN load for both linear and nonlinear models, then displacement are reached about 55 mm for nonlinear model. In addition, as is seen in Fig. 6b, displacements obtained from nonlinear model are higher

than those of linear model, and also displacements on the top point (K point see Fig 5.) are obtained as 35 mm and 55 mm, respectively from linear and nonlinear models.

Sx stress contour diagrams are presented for both linear and nonlinear models in Figs. 7(a)-7(b), respectively. When considered the whole of the columns, the stresses are lower than 3 MPa for linear model and 2 MPa for nonlinear model. However, the biggest values of the stresses are higher than the strength of the columns. On the other hand lower stresses are occurred in nonlinear model compared the linear model results.

Maximum stress-strain relation obtained from L point (See Fig. 5) is presented in Fig. 8(a) and the minimum stress-strain relation obtained from L' point (See Fig. 5) is presented in Fig. 8(b). It is clearly seen form Fig. 8 that the RCC column is both of cracked in tension and crushed in compression after yielding for nonlinear model. However, it is appeared that the stresses are exceeded the strength of material for linear model. The force-stress relation obtained on L' and L points are plotted in Figs. 9(a) and 9(b), respectively. As is seen in Fig. 9, the stresses are stable after 50 kN load for nonlinear model.

It is generally appeared from linear and nonlinear analyses of RCC column that, the nonlinear behavior is more suitable and realistic than linear behavior.
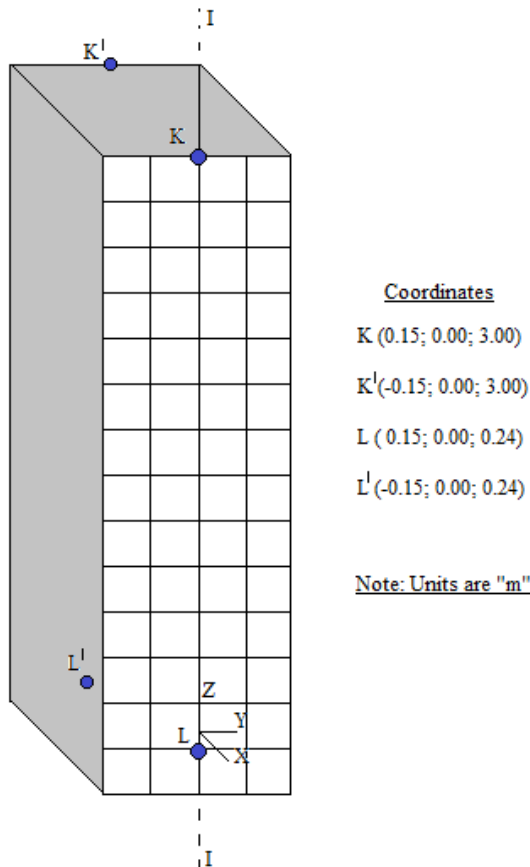
3.3.2 Finite element results of FCFRST column

The force-displacement curve and displacement changing along to height of the column are plotted in Figs. 10(a) and 10(b), respectively. It is stated from Fig. 10(a) that maximum displacement on K point is obtained from nonlinear model at about 1520 kN lateral load. As is seen in Fig. 10(a), 120 mm displacement occurs from nonlinear model when it is about 23 mm on linear model. According to Fig. 10(b), the displacements are increased along to height of the column for each linear and nonlinear model. However, the displacement on the top of the nonlinear model is reached about five times of this of linear model.

Sx contour diagrams obtained from linear and nonlinear analyses of FCFRST column are illustrated in Figs. 11(a) and 11(b), respectively. Although stresses obtained from nonlinear model are bigger than those of linear model, both of models provide safety considered strength of steel and concrete.
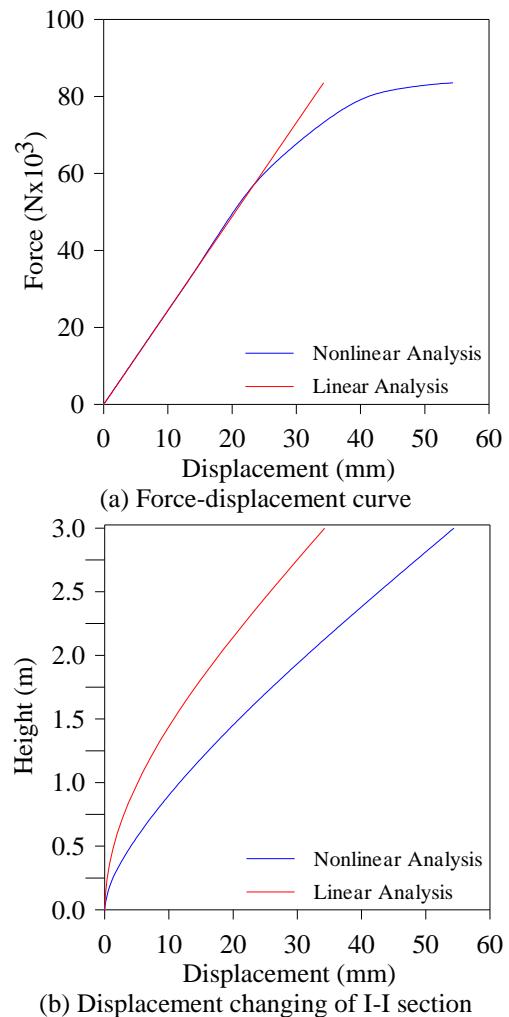

Coordinates

K (0.15; 0.00; 3.00)

K' (-0.15; 0.00; 3.00)

L (0.15; 0.00; 0.24)

L' (-0.15; 0.00; 0.24)

Note: Units are "m"

Fig. 5 Schematic view of points and sections

(a) Force-displacement curve

(b) Displacement changing of I-I section

Fig. 6 (a) Force-displacement curve on K point and (b) changing of displacements along to I-I- section obtained from RCR models
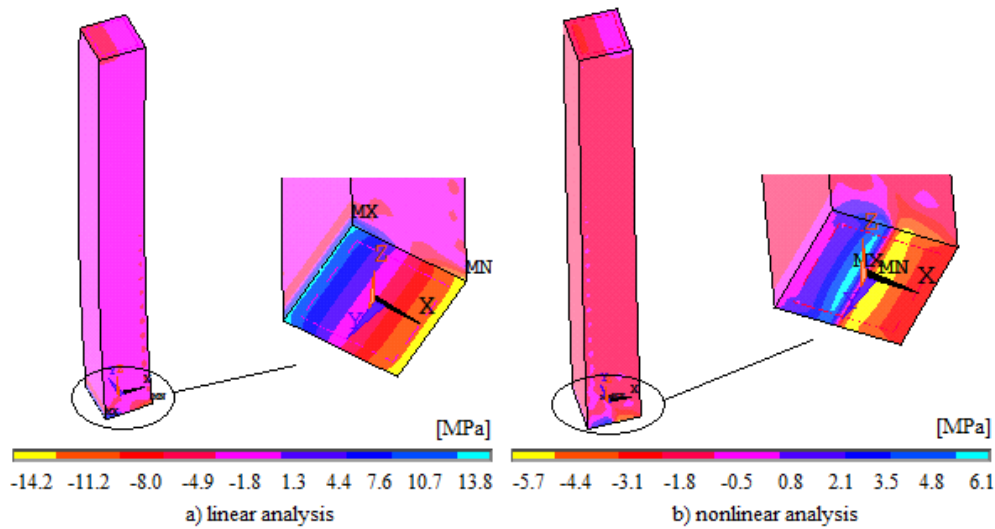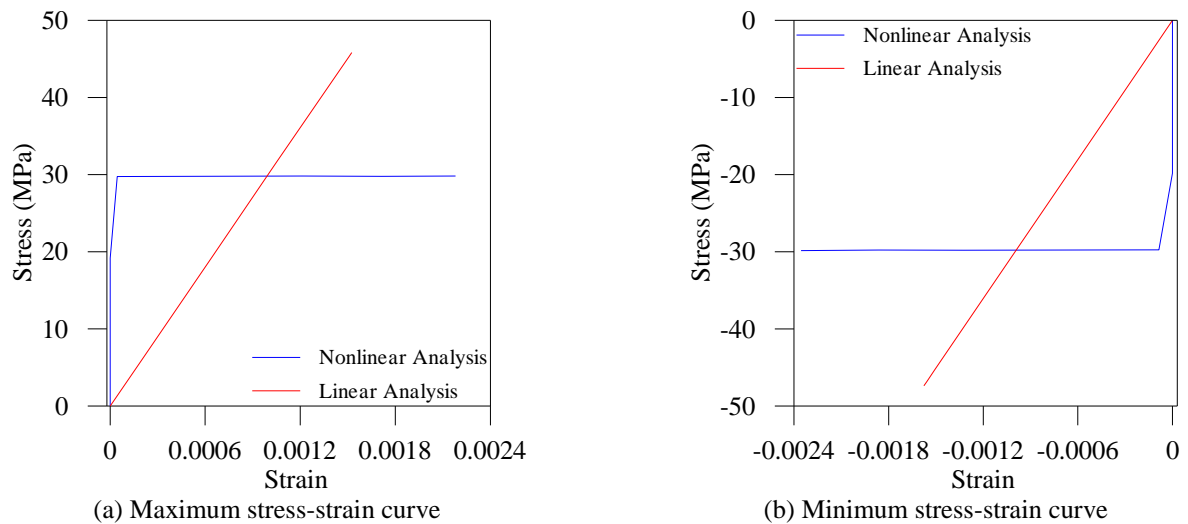
Fig. 7 S_x stresses obtained from analyses of RCR column

(a) Maximum stress-strain curve (b) Minimum stress-strain curve

Fig. 8 (a) Maximum stress-strain curve on L' point and (b) Minimum stress-strain curve on L point obtained from RCR models
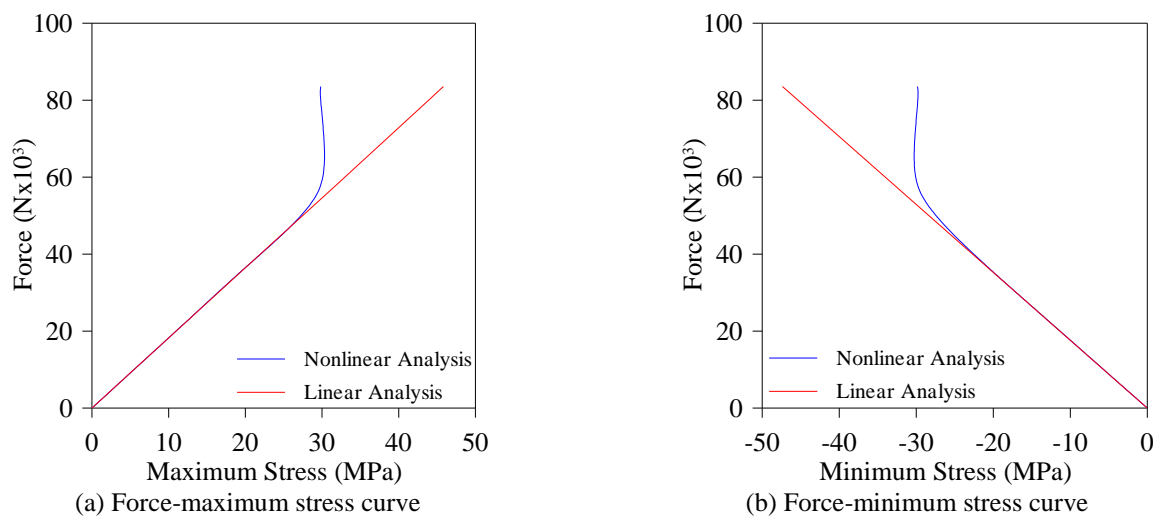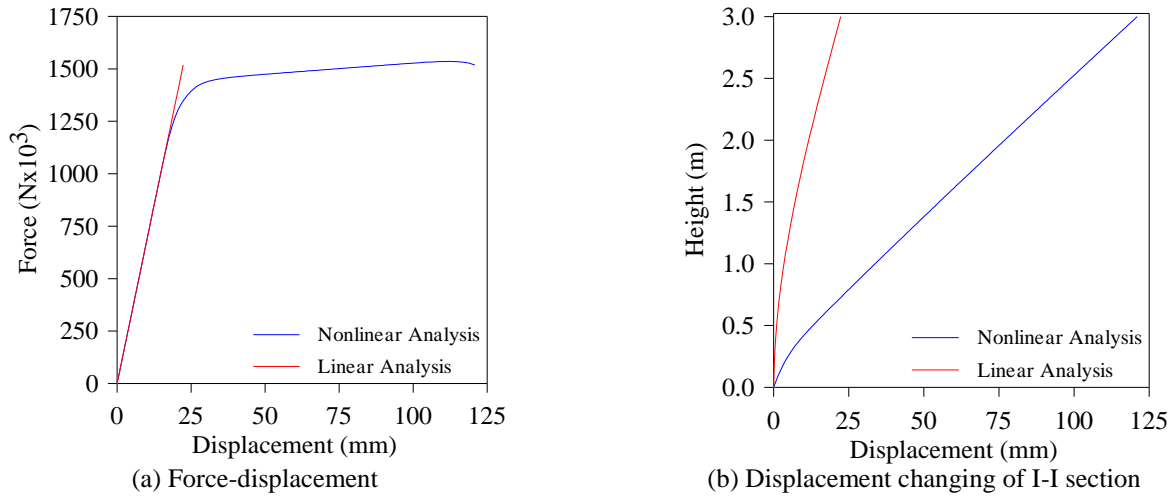

(a) Force-maximum stress curve (b) Force-minimum stress curve

Fig. 9 (a) Force-maximum stress curve on L' point and (b) Force-minimum stress curve on L point obtained from RCR models

(a) Force-displacement

(b) Displacement changing of I-I section

Fig. 10 (a) Force-displacement curve on K point and (b) changing of displacements along to I-I- section obtained from FCFRST models

a) linear analysis
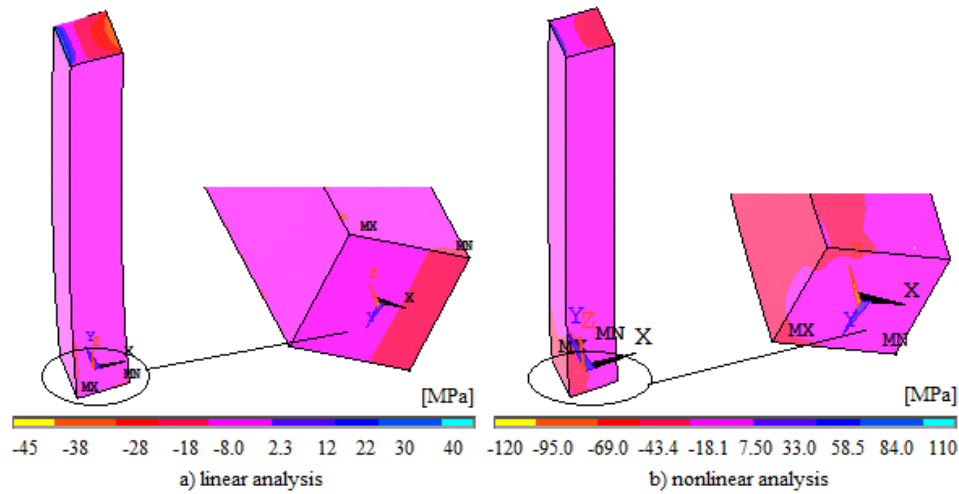
b) nonlinear analysis

Fig. 11 Sx stresses obtained from analyses of FCFRST column

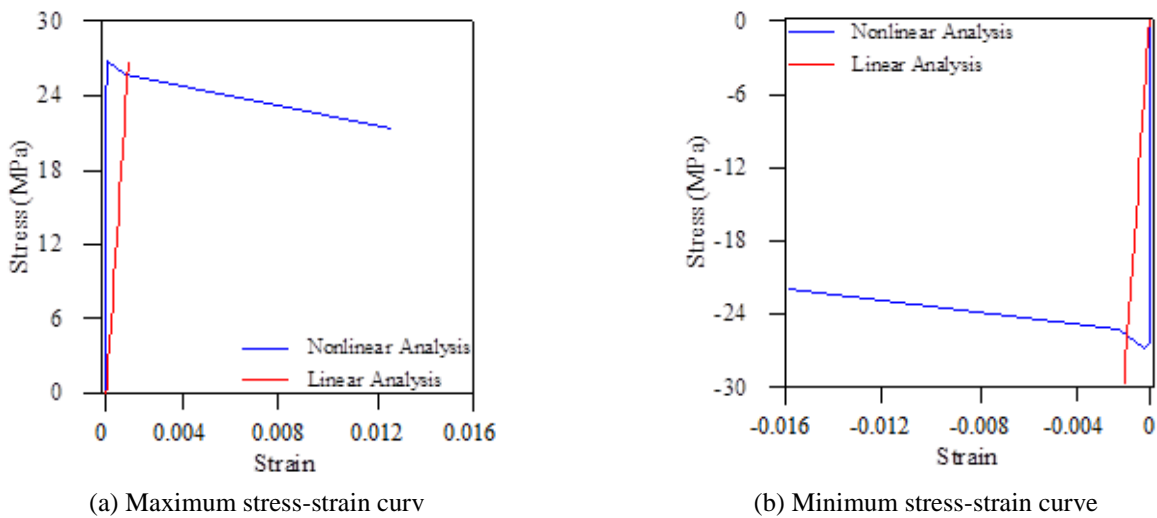(a) Maximum stress-strain curv

(b) Minimum stress-strain curve

Fig. 12 (a) Max. stress-strain curve on L' point and (b) Min. stress-strain curve on L point obtained from FCFRST models

(a) Force-maximum stress curve

(b) Force-minimum stress curve
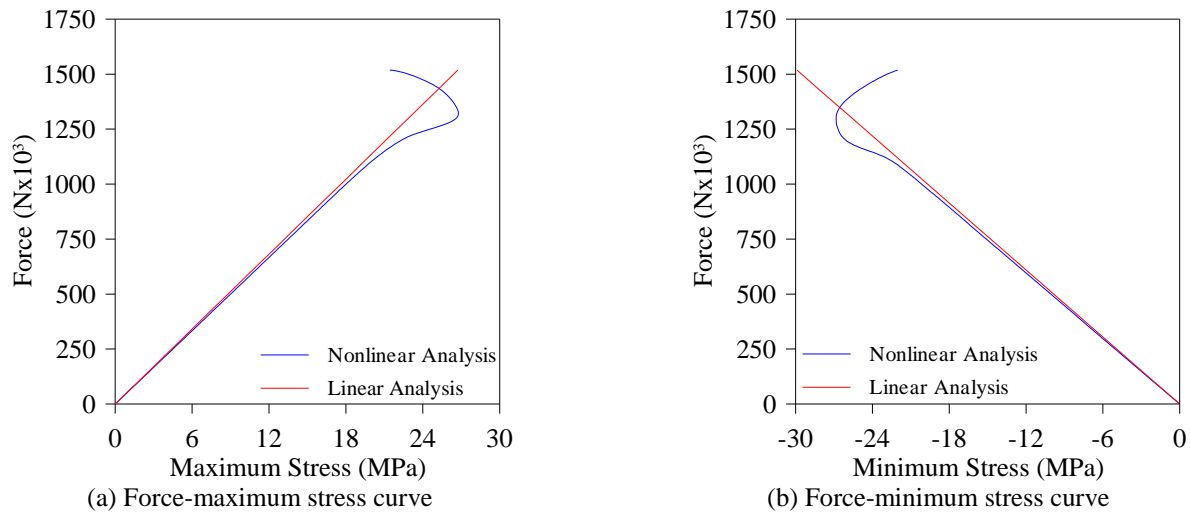
Fig. 13 (a) Force-max. stress curve on L' point and (b) Force-min. stress curve on L point obtained from FCFRST models

(a) Force-displacement curve
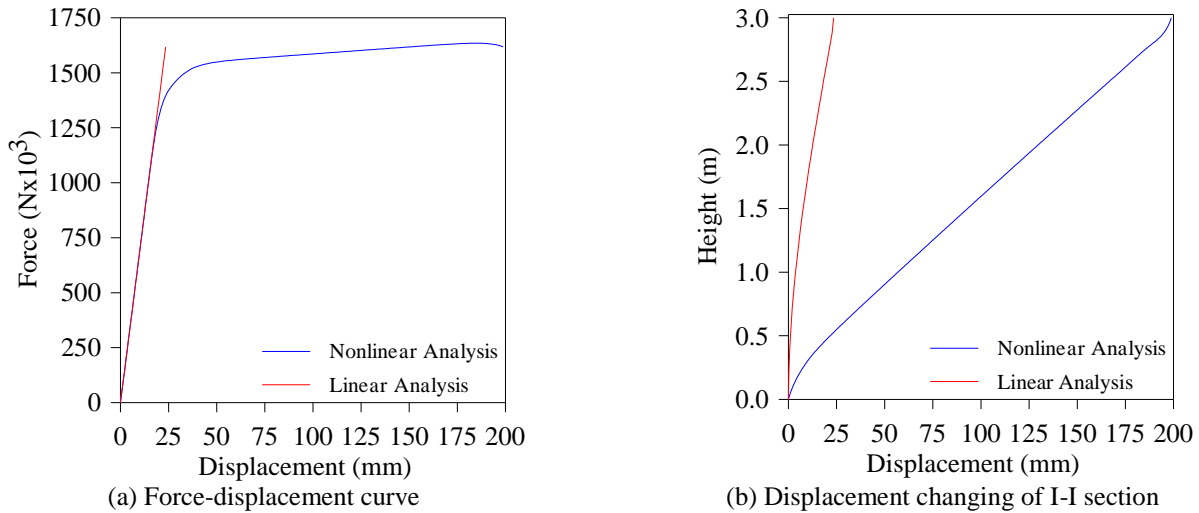
(b) Displacement changing of I-I section

Fig. 14 (a) Force-displacement curve on K point and (b) changing of displacements along to I-I- section obtained from CFDSRST models

Maximum and minimum stress-strain curves are plotted in Figs. 12(a) and 12(b), respectively obtained from linear and nonlinear analyses of the FCFRST column. It is indicated in Fig. 12 that the column behaves nonlinearly after 25 MPa and plastic strain is occurred on the system. Also ultimate plastic strain value is about seven times of the elastic strain. This shows that the column has high ductility. The force-stress relation obtained on L' and L points are plotted in Figs. 13(a) and 13(b), respectively. As is seen in Fig. 13, the stresses decrease after 1250 kN load for nonlinear model. This mean is that the nonlinear material is started to yield after 1100 kN load and the material is hardened about 1250 kN and it is braked about 1500 kN.

3.3.3 Finite element results of CFDSRST column

The force-displacement curve and displacement changing along to height of the column are plotted in Figs. 14(a) and 14(b), respectively which are obtained from linear

and nonlinear analyses of FCFRST column. It is stated from Fig. 14(a) that maximum displacement on K point is obtained as 200 mm from nonlinear model at about 1620 kN lateral load. However, the maximum displacement is about 23 mm obtained from linear model. On the other hand, the displacements increase through the height of the column, but the maximum displacement obtained from nonlinear model is about eight times of those of linear model.

Sx contour diagrams obtained from linear and nonlinear analyses are shown in Figs. 15(a) and 15(b), respectively. As is seen from Fig. 15 that extreme values are obtained at the top and the bottom of the column around the steel tube. The stress values are similar to those of FCFRST models.

Maximum and minimum stress-strain curves are plotted in Figs. 16(a) and 16(b), respectively obtained from linear and nonlinear analyses of the FCFRST column. The results look alike to those of FCFRST models.
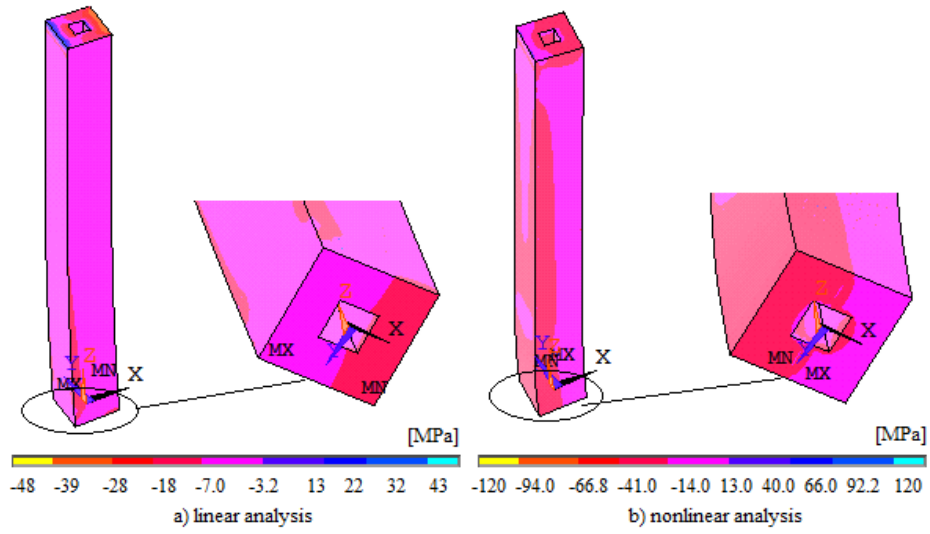
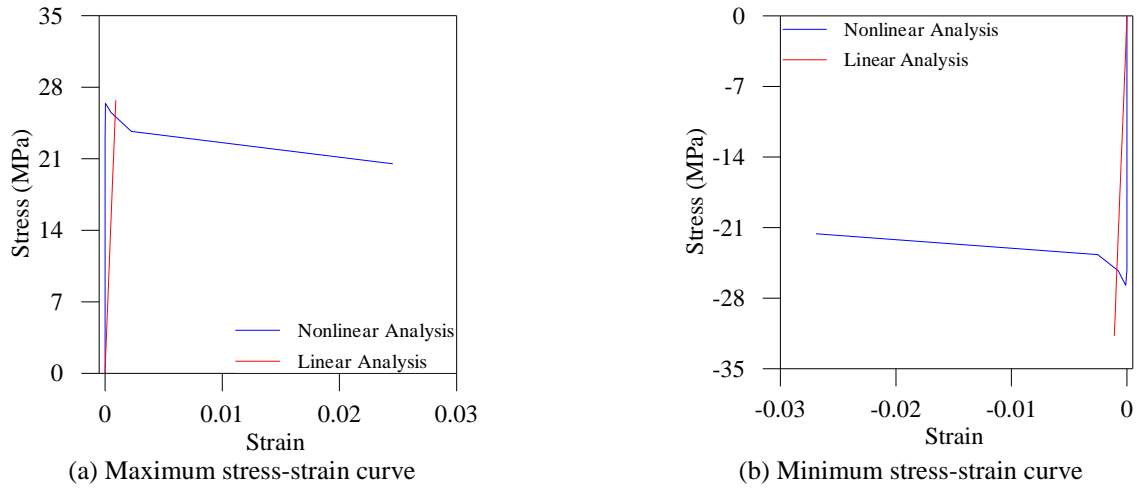Fig. 15 S_x stresses obtained from analyses of CFDSRST column

(a) Maximum stress-strain curve   (b) Minimum stress-strain curve

Fig. 16 (a) Max. stress-strain curve on L' point and (b) Min. stress-strain curve on L point obtained from CFDSRST models

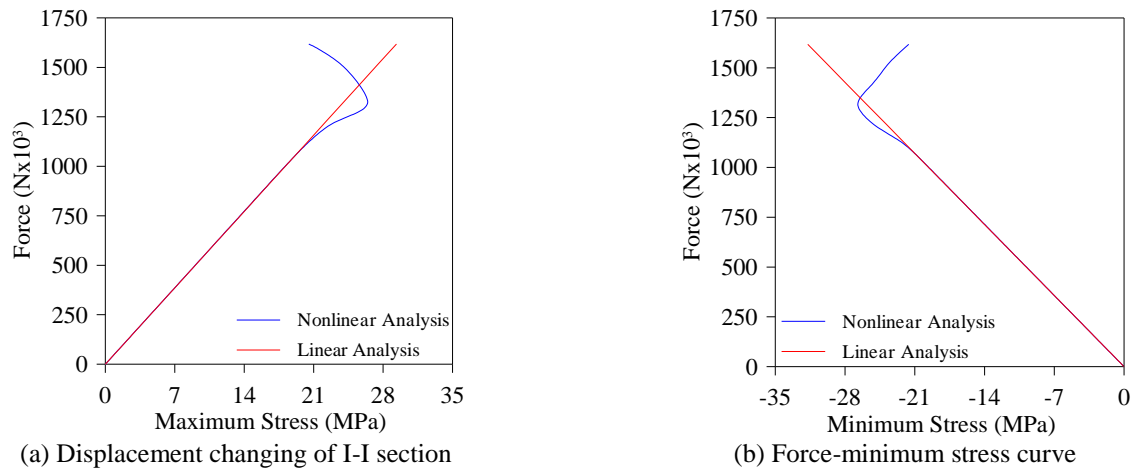
(a) Displacement changing of I-I section   (b) Force-minimum stress curve

Fig. 17 (a) Force-max. stress curve on L' point and (b) Force-min. stress curve on L point obtained from CFDSRST models

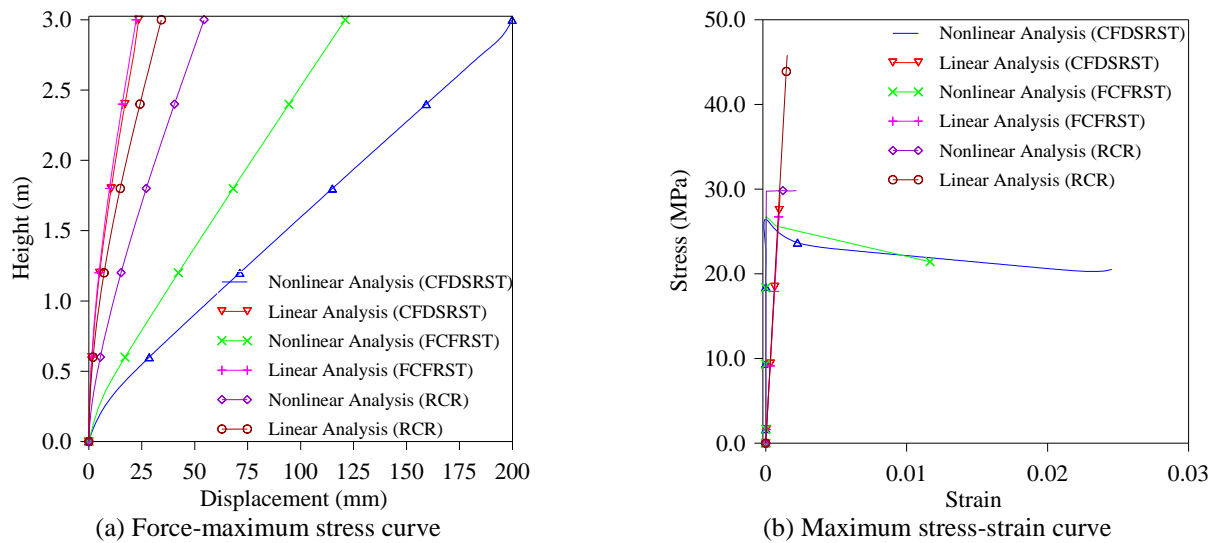(a) Force-maximum stress curve   (b) Maximum stress-strain curve

Fig. 18 (a) Changing of displacements along to I-I- section and (b) maximum stress-strain curve on L' point obtained from CFDSRST, FCFRST and RCR models

The force-stress relation obtained on L' and L points are plotted in Figs. 17(a) and 17(b), respectively. As is seen in Fig. 17, the stresses are similar to those of FCFRST models with a difference where the material is braked about 1600 kN.

3.3.4 Comparison of finite element results of the composite columns

In the study, linear and nonlinear analyses results of the RCR, FCFRST, and CFDSRST columns are separately presented. But it is necessary considering the analyses results together to make a clear evaluation. So displacement changings along to I-I section obtained from three different columns for linear and nonlinear analyses are plotted in Fig. 18(a). As is seen in Fig. 18(a), the displacements are increased along to height for all models and columns. As is also understood from Fig. 18(a), the maximum displacements are respectively obtained from nonlinear models of CFDSRST, FCFRST, and RCR models. In addition the maximum displacement obtained from nonlinear model of CFDSRST column is more than one and a half, four times those of nonlinear models of FCFRST and RCR, respectively. On the other hand, the maximum displacements obtained from linear analyses of linear CFDSRST and FCFRSR columns are similar to each other. But the value obtained from RCR model is a little bigger than this of CFDSRST and FCFRST models. The maximum stress-strain graphs are given in Fig. 18(b). As is seen from Fig. 18(b), the maximum strains are nearly obtained between 20-30 MPa except linear result of RCR column which is about 45 MPa. However it is commented that the linear model of the RCR column is cracked under such a load. On the other hand the maximum strains are obtained from nonlinear model of CFDSRST and FCFRST columns, respectively.

4. Conclusions

This study investigates the structural response of rectangular composite columns under vertical and lateral loads. For the purpose, a reinforced concrete rectangular column, a full concrete filled circular steel tube column and, a concrete filled double-skin rectangular-circular steel tube column are 3D constituted in ANSYS software considering both of linear and nonlinear models. Vertical and lateral loads are statically applied to models and displacement, stress, strain results are obtained. According to the study fallowing conclusions are obtained:

✓ The displacements are increased along the height of the all columns for both linear and nonlinear model. The displacements obtained from nonlinear models are bigger than those of linear models. The maximum displacement is obtained at the top point from nonlinear model of CFDSRST column which is more than one and a half, four times those of nonlinear models of FCFRST and RCR, respectively.

✓ The displacements are increased linear elastically increasing the lateral load. However the displacements are suddenly increased after maximum loading for nonlinear models. The maximum displacement obtained from nonlinear models of RCR, FCFRST and CFDSRST columns are nearly twice, five, and eight times bigger than those of RCR, FCFRST and CFDSRST columns, respectively.

✓ The stresses are nearly twice decreased obtained from nonlinear model of RCR column than those of linear model. On the other hand the maximum stresses obtained from linear model of the RCR column exceeds the tensile strength of the concrete material. Contrary to this, extreme stresses obtained from nonlinear models of FCFRST and CFDSRST columns are nearly three times bigger than those of linear models. The extreme stresses occurred on FCFRST

and CFDSRST columns are nearly around the steel tubes, but they do not exceed the strength of steel material.

✓ The ultimate strains under ultimate stresses obtained from nonlinear models of the RCR is nearly twice bigger than this of linear model. But the ratio is about twelve when considering nonlinear and linear ultimate strains obtained from and FCFRST and CFDSRST columns

✓ When considering three columns together, FCFRST and CFDSRST columns provide more and more safety, ductility compared to RCR column. On the other hand, CFDSRST column provides a little more safety and ductility according to FCFRST column.

✓ The both of displacements and stresses results are showed that nonlinear models are realistic far more than linear models.

References

Ajel, H.A. and Abbas, A.M. (2016), "Experimental and analytical investigations of composite stub columns", *Int. J. Innovative Res. Sci. Eng Tech.*, **4**(2), 185-200.

Alnahhal, W. and Aref, A. (2008), "Structural performance of hybrid fiber reinforced polymer–concrete bridge superstructure systems", *Compos. Struct.,* **84**(4), 319-336.

ANSYS 2016, Swanson Analysis System, USA.

Aslani, F., Uy, B., Wang, Z. and Patel, V. (2016), "Confinement models for high strength short square and rectangular concrete-filled steel tubular columns", *Steel Compos. Struct.*, **22**(5), 937-974.

Bouazaoui, L., Perrenot, G., Delmas, Y. and Li, A. (2007), "Experimental study of bonded steel concrete composite structures", *J. Constr. Steel. Res.*, **63**(9), 1268-1278.

Chacon, R. (2015), "Circular concrete-filled tubular columns: state of the art oriented to the vulnerability assessment", *Open Civ. Eng. J.,* **9**, 249-259.

Chen, Z., Lei, J. and Zheng, Z. (2008), Research on CCRST columns used in seismic regions", *Proceedings of the 14 th World Conference on Earthquake Engineering*, Beijing, China, October.

Essopjee, Y. and Dundu, Y.M. (2015), "Performance of concrete-filled double-skin circular tubes in compression", *Compos. Struct.,* **133**, 1276-1283.

Eurocode 4, EN 1994-1-1 (2004), Design of Composite Steel And Concrete Structures, European Committee For Standardization, Brussel, Belgium.

Fakharifar, M., Chen, G., Lin, Z. and Woolsey, Z.T. (2014), "Behavior and strength of passively confined concrete filled tubes", *Proceedings of the 10th National Conference in Earthquake Engineering*, Earthquake Engineering, Research Institute, Anchorage.

Furlong, R. (1997), "Steel-concrete composite columns", Transportation Research Record: *Journal of the Transportation Research Board*, **1594**, 57-63.

Guo, W.X., Ruofei, H.Q.Z., Xinyu, Z. and Qun, Y. (2014), "Structural behaviors of sustainable hybrid columns under compression and flexure", *Struct. Eng. Mech.*, **52**(5), 857-873.

Ha, S.K., Na, S. and Lee, H.K. (2013), "Bond characteristics of sprayed frp composites bonded to concrete substrate considering various concrete surface conditions", *Compos. Struct.*, **100**, 270-279.

Hajjar, J.F. (2002), "Composite steel and concrete structural systems for seismic engineering", *J. Constr. Steel. Res.*, **58**(5-8), 703-723.

Huang, Z., Jiang, L.Z., Zhou, WB. and Chen, S. (2016), "Studies

on restoring force model of concrete filled steel tubular laced column to composite box-beam connections", *Steel Compos. Struct.*, **22**(6), 1217-1238.

Jacobs, W.P. and Hajjar, J.F. (2010), "Load transfer in composite construction", *2010 Structures Congress*, Orlando, May.

Kachlakev, D. and Miller. T (2001), "Finite element modelling of concrete structures strengthened with FRP laminates", Final Report, SPR316, Oregon Department of Transportation Research Group, Salem.

Karimi, K., Tait, M.J. and El-Dakhakhni, W.W. (2011), "Testing and modeling of a novel FRP-encased steel-concrete composite column", *Compos. Struct.*, **93**(5), 1463-1473.

Kisala, D. (2016), "A finite element analysis of steel plate–concrete composite beams including the influence of stiffness of the connectors on deflection", *Technical Transactions, Civil Engineering*, DOI: 10.4467/2353737XCT.16.159.5770, 69-80.

Li, J. and Hadi, M.N.S. (2003), "Behaviour of externally confined high-strength concrete columns under eccentric loading", *Compos. Struct.*, **6,** 145-153.

Liu, J. (2013). "Neural networks method applied to the property study of steel-concrete composite columns under axial compression", *Int. J. Smart Sens. Intel. Syst.*, **6**(2), 548-566.

Oyawa, W.O., Gathimba, N.K. and Mang'uriu, G.N. (2016), "Structural response of composite concrete filled plastic tubes in compression", *Steel Compos. Struct.*, **21**(3), 589-604.

Patel, V. and Lande, P.S. (2016), "Analytical behavior of concrete filled steel tubular columns under axial compression", *Int. J. Eng. Res.*, **5**(3), 629-632.

Patidar, A.K. (2012), "Behaviour of concrete filled rectangular steel tube column". *IOSR J. Mech. Civ. Eng.*, **4**(2), 46-52.

Pecce, M. and Ceroni, F. (2010), "Bond tests of partially encased composite columns", *Adv. Steel Constr.*, **6**(4), 1001-1018.

Pereira, M.F., Nardin, S.D. and Debs, A.L.H.C. (2016), "Structural behavior of partially encased composite columns under axial loads", *Steel Compos. Struct.*, **20**(6), 1305-1322.

Remennikov, A.M. and Kong, S.Y. (2012), "Numerical simulation and validation of impact response of axially-restrained steel-concrete-steel sandwich panels", *Compos. Struct.*, **94**(12), 3546-3555.

Robinson, M.J. and Melby, I.H. (2015), "Effects of bonding in short-span rectangular concrete filled GFRP tubes", *Compos. Struct.*, **133**, 131-139.

Sakino, K., Nakahara, H., Morino, S. and Nishiyama, I. (20049, "Behavior of centrally loaded concrete-filled steel-tube short columns", *J. Struct. Eng.*, **130**(2), 180-188.

Schneider, S.P. (1998), "Axially loaded concrete-filled steel tubes", *J. Struct. Eng.*, **124**(10), 1125-1138.

Uenaka, K., Kitoh, H. and Sonoda, K. (2010), "Concrete filled double skin circular stub columns under compression", *Thin Wall. Struct.*, **48**(1), 19-24.

Wei, S., Mau, S.T., Vipulanandan, C. and Mantrala, S.K. (1995), "Performance of newsandwich tube under axial loading: experiment", *J. Struct. Eng.*, **121**(12), 1806-1814.

Wu, X.G., Zou, R., Zhao, X. and Yu, Q. (2015), "Theoretical study of UHPCC composite column behaviors under axial compression", *Struct.Eng. Mech.*, **55**(5), 931-951.

Zhao, H. (2016), "Analysis of seismic behavior of composite frame structures", *Steel Compos. Struct.*, **20**(3), 719-729.

CC